Magnetochemical and Molecular Orbital Analyses on Lithium Electrochemically Doped Non-Graphitizable Carbon Electrode of Lithium Ion Rechargeable Batteries

Koichi TANAKA,* Masafumi ATA, Hitoshi KIMURA, and Hiroshi IMOTO†
Sony Corporation Research Center, 174 Fujitsuka-cho, Hodogaya-ku, Yokohama 240
†R&D Division, Sony Corporation Battery Group, 174 Fujitsuka-cho, Hodogaya-ku, Yokohama 240
(Received March 8, 1994)

The electronic characteristics of electrochemically doped lithium in non-graphitizable carbon, which was obtained by heat-treating polyfurfuryl alcohol (PFA-C) and was used as the negative electrode of lithium ion rechargeable batteries, were examined with the aid of ^{7}Li solid-state nuclear magnetic resonance (NMR) and electron spin resonance (ESR). In order to clarify how lithium is incorporated in the carbon electrode, discrete variational-$X\alpha$ (DV-Xα) molecular-orbital calculations were also performed on a model system. These experimental and theoretical results suggest that the lithium doped in the carbon exists in a non-metallic state with low electron density as compared to the ionic crystal, and that the unpaired electrons in the lithium doped carbon are delocalized at the peripheral carbon domains of the system. This was theoretically supported by the fact that the singly occupied molecular orbital (SOMO) of the lithium doped carbon is lower by 5.388 eV than the orbital localized predominantly on lithium 2s, and that the system is stabilized by electron donation from lithium to the carbon.

Lithium ion rechargeable batteries are known to be extremely safe and more reliable than rechargeable batteries with lithium metal. This is because the charge–discharge reaction between a carbon negative electrode and a positive electrode consisting of a metallic composite oxide such as lithium cobalt dioxide ($LiCoO_2$) deals only with the lithium ion. They are also comparable in energy density to metallic lithium rechargeable batteries. Therefore, these new high-performance batteries have rapidly become popular as the electric power source for portable electronic equipment such as cellular phones, camcorders and so on. Since a carbon electrode with high capacity and good reversibility during charging and discharging is required in order to attain a high energy density and many charge cycles, many types of carbonaceous materials have been developed recently.[1—13] We have also developed a new carbonaceous material by the heat-treatment of polyfurfuryl alcohol, which is a form of non-graphitizable carbon (PFA-C), and have obtained higher performance than conventional materials.[14,15] However, the electronic state of the doped lithium in a non-graphitizable carbon electrode such as PFA-C has not been sufficiently analyzed.

In this paper, we report some novel results obtained using solid-state nuclear magnetic resonance (solid-state NMR) and electron spin resonance (ESR). We also describe some theoretical predictions based on molecular-orbital calculations.

Experimental

PFA-C, which was used as an electrode, was obtained by heat-treating polyfurfuryl alcohol at 1100 °C under a nitrogen atmosphere. The electrochemical doping of lithium into the carbon electrode was performed in propylene carbonate (PC) electrolyte solution dissolved in 1 mol dm^{-3} of lithium hexafluorophosphate ($LiPF_6$) by passing an electric current of 0.5 mA cm^{-2} into metallic lithium as a counter electrode. The lithium doping rate were set at 45, 90, and 100% of the maximum capability of the carbon. The carbon electrodes were washed after the electrochemical doping with 1, 2-dimethyoxyethane (DME) to eliminate $LiPF_6$, and then dried under vacuum. All the processes were done under an argon atmosphere with a dew point of under −60 °C and an oxygen concentration of less than 0.1%.

^{7}Li solid-state NMR spectra were observed at 25 °C using a JEOL NM-GSX270MU/VT solid-state high resolution NMR spectrometer. The actual measurements were carried out by adopting a magic angle spinning of 6000 rpm. ESR spectra were observed at 25 °C using a JEOL JES-RE2X X-band ESR spectrometer with a 100 kHz field modulation. The field modulation was maintained below 0.01 mT, and the microwave power was fairly low to avoid power saturation. The molecular orbital calculations were performed using an ALLIANT FX/2800GT mini-super computer.

Results and Discussion

^{7}Li Solid-State NMR Studies. We performed ^{7}Li solid-state NMR analysis to obtain the Knight shifts of the lithium doped in the carbon electrode. The resonance frequency shift in NMR is usually represented by

$$\Delta H/H = -8\pi/3 \cdot \chi/n \cdot \rho(\mathrm{N}), \quad (1)$$

where χ is magnetic susceptibility of electron spin, n is the spin concentration and ρ (N) is the electron spin density at the atomic nucleus.[16] Therefore, the shift is related to the product of electron spin susceptibility and electron spin density. The electron spin susceptibility in Eq. 1 is represented by

$$\chi/n = [g^2\beta^2 s(s+1)]/3kT. \quad (2)$$

We can consider the equation to be a function of temperature T, because the g-value, Bohr magneton β, spin quantum number s and Boltzmann constant k are con-

stant in the examination. Consequently, when the temperature under determination is constant, the resonance frequency shift is proportional to the electron spin density at the atomic nucleus. We can predict the electron density at the lithium nucleus by determining the frequency shift of lithium doped in the carbon, the Knight shift. Knight shifts were obtained in relation to the resonance frequency of metallic lithium.

The observed ^{7}Li solid-state NMR spectra of the samples are shown in Fig. 1. The spectrum of lithium chloride, which is a typical ionic crystal, is shown in Fig. 2. The Knight shifts of these samples are collected in Table 1. The same investigation was carried out on carbon which was not doped with lithium. No magnetic absorption attributable to lithium was observed. These observations suggest that lithium from the electrolyte

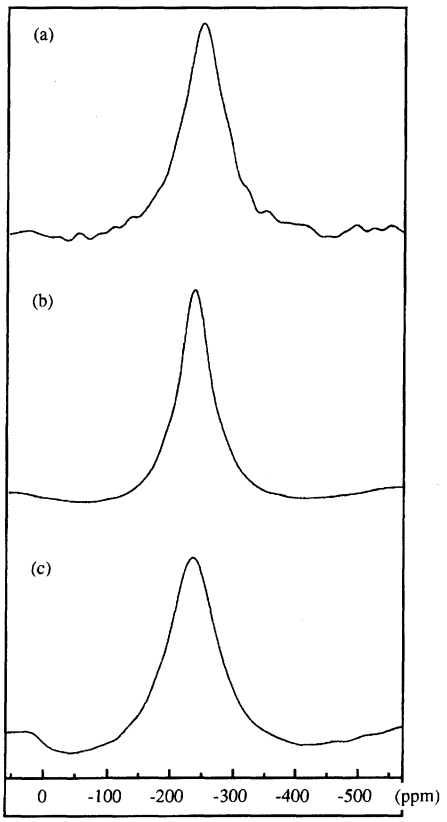

Fig. 1. ^{7}Li solid-state NMR spectra of the lithium doped carbons observed at 25 °C. The lithium doping rate was (a) 45%, (b) 90%, and (c) 100% of the maximum capability of the carbon. The resonance frequency of metallic lithium was set at 0 ppm.

Table 1. Knight Shifts of ^{7}Li Nuclei in the Lithium Doped Carbons Observed at 25 °C

Doping rate (%)	Knight shift (ppm)
45	−250.05
90	−239.19
100	−236.43
LiCl (ionic crystal)	−256.01

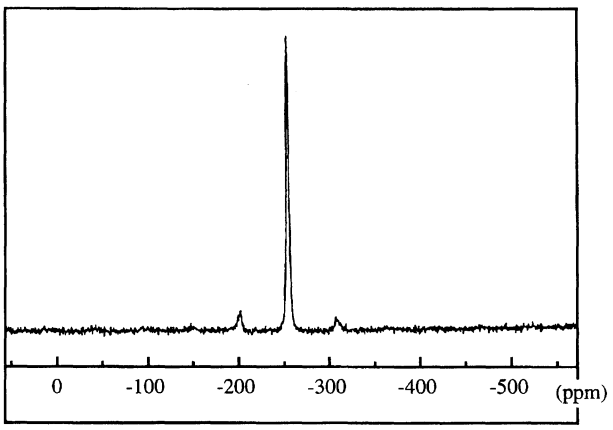

Fig. 2. ^{7}Li solid-state NMR spectrum of lithium chloride observed at 25 °C. The resonance frequency of metallic lithium was set at 0 ppm.

solution did not remain in the investigated samples. All shift values recorded for lithium in the carbon were essentially identical to that of lithium in the ionic crystal. This suggests that the electron density at the lithium nucleus in the lithium doped carbon is as low as that of the ionic crystal. The shift seemed to decrease with increasing doping rate. However, it is not clear at present whether this tendency shows the increase in the electron density at the lithium nucleus with increasing the doping rate or not. Moreover, all the spectra of the lithium doped carbon were broader than those of lithium chloride. The broading of the absorption line may be caused by not only the quickness of paramagnetic relaxation due to an unpaired electron, but also the delocalization of the electron spin in the carbon domain. In addition, it is predicted that there is a variation in the carbon structure which would change the electron density in the carbon. Consequently, it was confirmed that the doped lithium exits in a non-metallic state with low electron density up to the fully doped case.

ESR Studies. Using ESR it is possible to obtain several clues of how the unpaired electrons exist. In other words, it is possible to predict whether the electrons injected into the carbon electrode from the positive one through the outer circuit are localized around the lithium nuclei or delocalized in the carbon domain. The ESR spectra of the lithium doped carbon are shown in Fig. 3. As can be seen from this figure, the spectra consisted of only one strong sinusoidal line. The center of the resonance magnetic field in ESR is given in the g-value. The g-value is obtained by simultaneous measurement with digital Mn^{2+} marker as the reference, and using the relationship

$$g = g_s(1 - \Delta H/H_0), \tag{3}$$

based on the resonance magnetic field of the fourth peak from the lower field in six peaks of the Mn^{2+} marker, where g_s is the g-value of the peak in the marker (1.981), H_0 is the resonance field of the reference peak and ΔH

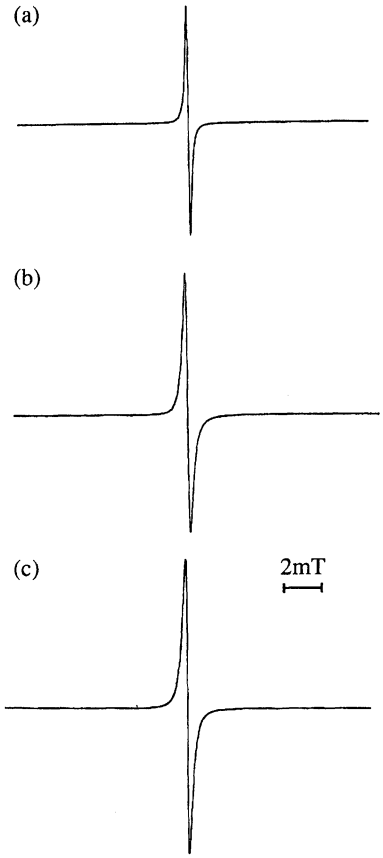

Fig. 3. ESR spectra of the lithium doped carbons observed at 25 °C. The lithium doping rate was (a) 45%, (b) 90%, and (c) 100% of the maximum capability of the carbon.

is the difference in resonance field between the reference peak and the absorption of the sample. In every case, the g-value was estimated to be 2.0027. They are close to the values for aromatic radicals. Accordingly, it could be considered that the unpaired electrons are delocalized in the carbon domain.

If the unpaired electrons exist near the lithium nuclei to cause a strong interaction between them, hyper fine structure should be observed in the spectra. However, such structure was not found in the investigations. Figure 4 shows the ESR spectrum measured at liquid helium temperature (4 K). The hyper fine structure could not be observed in this spectrum either. Consequently, the unpaired electron is undoubtedly delocalized in the peripheral carbon domain of lithium doped carbon, but not so close to the lithium nucleus that strong spin exchange interaction occurs.

For the carbon without lithium doping, the strong absorption as mentioned above was not observed. Therefore, those strong absorptions are evidently different from the absorption attributable to the dangling bonds at the ends of the carbon domain, which is relatively weak and broad.

Metallic lithium which has an unpaired electron in the outermost shell also causes ESR absorption. The

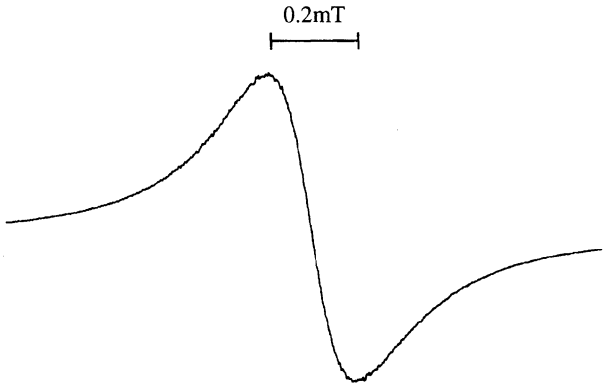

Fig. 4. ESR spectrum of the lithium 100%-doped carbon observed at liquid helium temperature (4 K).

spectrum of metallic lithium is shown in Fig. 5. It is already proved from the NMR results that the doped lithium does not exist in metallic state. The g-value of metallic lithium is 2.0020 which is different from the value obtained from the previous examinations. It was suggested that the strong absorption for the lithium doped carbon was not caused by metallic lithium.

It could be estimated that the unpaired electrons tend to be delocalized at some distance from the lithium nuclei.

Molecular-Orbital Calculations. The molecular-orbital calculations were performed in order to theoretically consider the electronic state at the lithium nucleus doped in the carbon. The discrete variational-Xα (DV-Xα) Molecular-Orbital method, which is one of the nonempirical ones, was used for the calculations. It is in general possible to treat larger molecules using this method than using the ab-initio method. It has been also known to have high accuracy particularly about a model in the excited state or in the charge transfer state.[17,18] Accordingly, it is considered that the DV-Xα method is most suitable for our studies. In the DV-Xα method, the exchange-correlation term $\hat{V}_{\mathrm{x}}(\boldsymbol{r})$ in the one-electron Hamiltonian is written in terms of the statistical local potential

$$\hat{V}_{\mathrm{x}}(\boldsymbol{r}) = -3\alpha[(3/8\pi)\cdot\rho(\boldsymbol{r})]^{1/3}, \quad (4)$$

where $\rho(\boldsymbol{r})$ is the local electron density at $\boldsymbol{r}$. The coeffi-

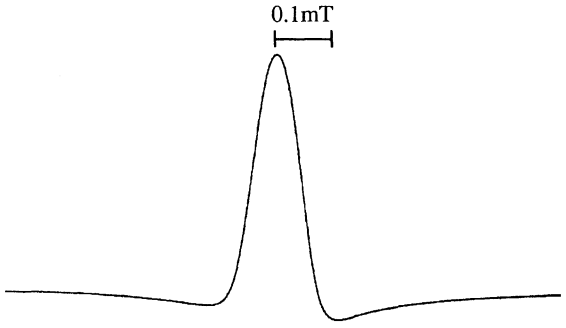

Fig. 5. ESR spectrum of metallic lithium observed at 25 °C.

cient α is the scaling parameter in the DV-Xα method and was set to $\alpha=0.7$ throughout the investigation. In the DV-Xα method, the ionization energy and the electron affinity are usually evaluated by Slater's transition-state method.[19]

The model of the lithium doped carbon for the calculations is shown in Fig. 6. In this model, the carbon layer consists of nineteen aromatic rings condensed in the configuration having six rotating axes. The dangling bonds at the outermost carbon atoms in the layer were terminated by hydrogen atoms. Then, two of the layer were stacked with a lithium atom centered between them. The bond length of C–C was 0.14 nm and that of C–H was 0.098 nm. The interlayer distance was 0.370 nm which was determined for lithium doped PFA-C using X-ray diffraction analysis in the previous studies.[14,15]

From the calculations of the overlap populations, it was confirmed that lithium was unlikely to be linked with any of the carbon atoms. In the lithium–carbon system, the energy level of the singly occupied molecular orbital (SOMO) and that of the orbital localized predominantly on lithium 2s were compared. Figure 7 shows that there is little difference in energy between the lowest-unoccupied molecular orbital (LUMO) of free carbon and the 2s atomic orbital of free lithium. However, doping of a lithium in the carbon raises the energy of the orbital localized predominantly on lithium 2s and reduces that of the LUMO due to the electronic correlation between them. This results in difference between the orbital localized predominantly on lithium 2s and the SOMO of the system by 5.388 eV. Therefore, it was predicted that the lithium–carbon system becomes more stable when the electron on the lithium 2s atomic orbital moves to the LUMO of the carbon.

The schematic representation of the SOMO of the lithium doped carbon is shown in Fig. 8. Consequently, it was suggested that the unpaired electron tends to be delocalized at the peripheral carbon domains.

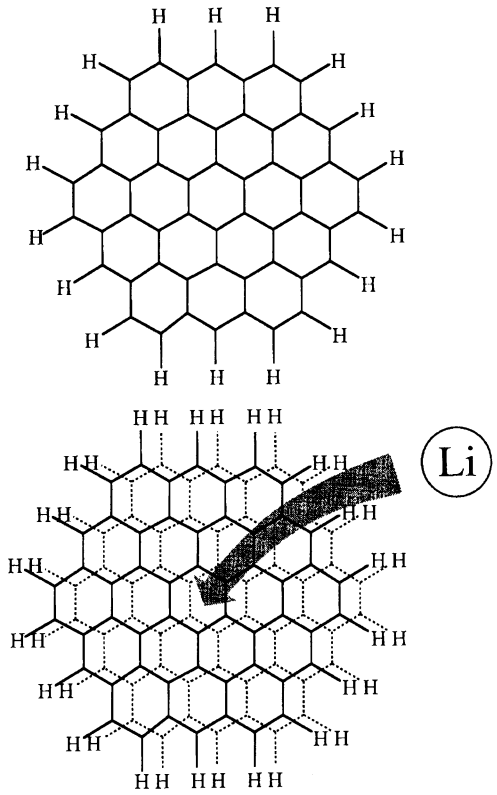

Fig. 6. Model of the lithium doped carbon used for the DV-Xα molecular-orbital calculations. C–C and C–H bond lengths were fixed to 0.140 and 0.098 nm, respectively, and the interlayer distance after setting a lithium atom at the center was set to 0.370 nm by referring to the X-ray diffraction data of the lithium doped carbon.

Summary

The following novel results were obtained;

(1) The lithium doped in the non-graphitizable carbon such as PFA-C exists in a non-metallic state with low electron density as compared to an ionic crystal such as lithium chloride.

(2) The unpaired electrons in the lithium doped carbon are delocalized at the peripheral carbon domains of the lithium doped carbon.

(3) By electrochemical doping of lithium to the carbon electrode, the electron on the lithium 2s orbital moves to the LUMO of the carbon because the energy level of

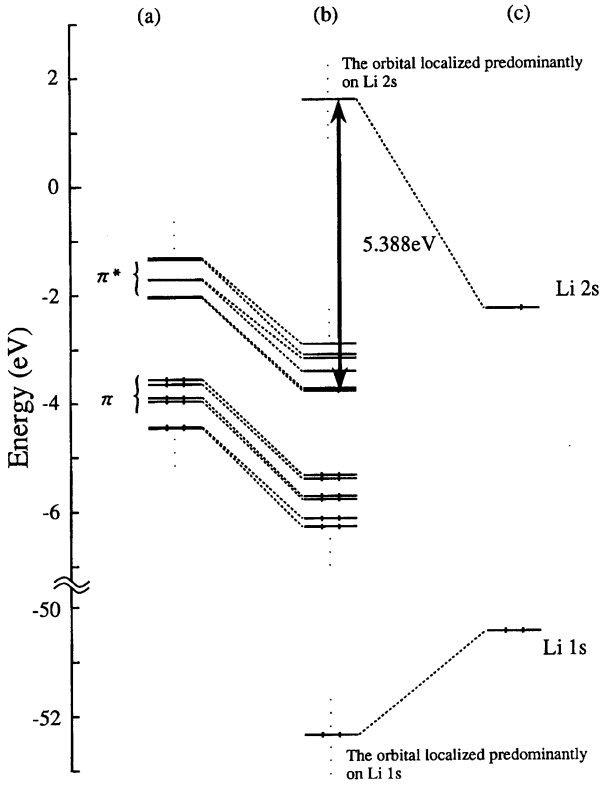

Fig. 7. Orbital-energy levels of (a) free carbon, (b) lithium doped carbon and (c) lithium free atom predicted by the DV-Xα molecular-orbital calculations.

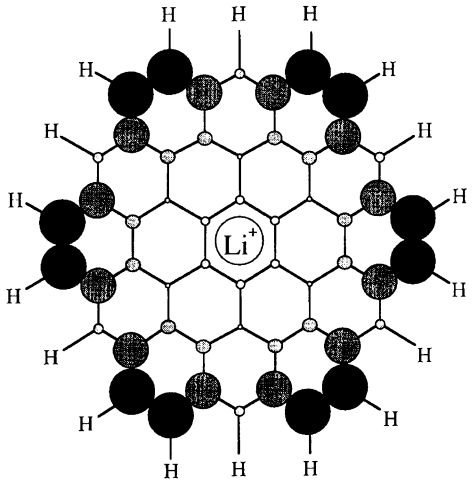

Fig. 8. Schematic representation of the singly occupied molecular orbital of the lithium doped carbon by the DV-Xα molecular-orbital calculations.

the SOMO of the lithium doped carbon is sufficiently lower than that of the orbital localized predominantly on lithium 2s.

References

1) K. Inada et al., *Denshi Jyoho Tsushin Gakkai Gijyutsu Kenkyu Hokoku* (*The Transactions of the Institute of Electronics, Information and Communication Engineers*), CPM 87-100 (1988).

2) K. Tanaka, M. Ueda, T. Koike, T. Yamabe, and S. Yata, *Synth. Met.*, **25**, 265 (1988).

3) M. Mohri, N. Yanagisawa, Y. Tajima, H. Tanaka, T. Mitate, S. Nakajima, M. Yoshida, Y. Yoshimoto, T. Suzuki, and H. Wada, *J. Power Sources*, **26**, 545 (1989).

4) R. Kanno, Y. Takeda, S. Ohashi, and O. Yamamoto, "30th Battery Symposium of Japan," Nagoya, 1989, Abstr., 1B12, p. 51.

5) T. Iijima, K. Suzuki, and M. Sato, "31st Battery Symposium of Japan," Osaka, 1990, Abstr., 3B09, p. 273.

6) T. Mitate, H. Tanaka, H. Kitayama, and K. Yamada, "31st Battery Symposium of Japan," Osaka, 1990, Abstr., 3B11, p. 277.

7) H. Imoto, H. Azuma, A. Omaru, and Y. Nishi, "58th Meeting of the Electrochemical Society of Japan," Noda, 1991, Abstr., 2F11, p. 158.

8) A. Omaru, H. Azuma, H. Imoto, and Y. Nishi, "58th Meeting of the Electrochemical Society of Japan," Noda, 1991, Abstr., 2F12, p. 158.

9) M. Ide, M. Mizutani, and M. Yamachi, "32nd Battery Symposium of Japan," Kyoto, 1991, Abstr., 2B12, p. 147.

10) J. Yamaura, Y. Ozaki, A. Morita, and A. Ohta, *J. Power Sources*, **43-44**, 233 (1993).

11) M. Fujimoto, N. Yoshinaga, K. Ueno, T. Nohma, M. Takahashi, I. Nakane, H. Watanabe, S. Yoshimura, K. Moriwaki, K. Nishio, and N. Furusawa, "59th Meeting of the Electrochemical Society of Japan," Hachioji, 1992, Abstr., 3J24, p. 239.

12) A. Mabuchi, C. Yamaguchi, H. Matsuyoshi, T. Kasuh, and T. Maeda, "33rd Battery Symposium of Japan," Tokyo, 1992, Abstr., 3A02, p. 191.

13) B. M. Way and J. R. Dahn, "182nd Meeting of the Electrochemical Society," Toronto, Canada, Oct. 11—16, 1992, Abstr., No. 30, p. 41.

14) A. Omaru, H. Azuma, M. Aoki, A. Kita, and Y. Nishi, "182nd Meeting of the Electrochemical Society," Toronto, Canada, Oct. 11—16, 1992, Abstr., No. 25, p. 34.

15) H. Imoto, A. Omaru, H. Azuma, and Y. Nishi, "182nd Meeting of the Electrochemical Society," Toronto, Canada, Oct. 11—16, 1992, Abstr., No. 26, p. 35.

16) C. P. Slichter, "Principles of Magnetic Resonance," 2nd ed, ed by M. Cardona, P. Fulde, and H-J Queisser, Springer-Verlag, Berlin, Heidelberg, and New York (1980), pp. 106—121.

17) A. Rosen, D. E. Ellis, H. Adachi, and F. W. Averill, *J. Chem. Phys.*, **65**, 3629 (1976).

18) H. Adachi, "Ryoshi Zairyo Kagaku Nyumon," Sankyo-Syuppan, Tokyo (1991).

19) J. C. Slater, J. B. Mann, T. M. Wilson, and J. H. Wood, *Phys, Rev.*, **184**, 672 (1969).